OPTICAL MICRORHEOLOGY OF SOFT COMPLEX MATERIALS

FRANK SCHEFFOLD[1], FRÉDÉRIC CARDINAUX,
SARA ROMER AND PETER SCHURTENBERGER

Department of Physics, University of Fribourg
CH-1700 Fribourg, Switzerland

SERGEY E. SKIPETROV

Laboratoire de Physique et Modélisation des Milieux Condensés
CNRS, F-38042 Grenoble, France

AND

LUCA CIPELLETTI

GDPC, Université Montpellier II
F-34095 Montpellier Cedex 05, France

Abstract. Dynamic multiple light scattering (diffusing wave spectroscopy, DWS) has been used to study the viscoelastic properties of soft materials. Several new multiple scattering approaches were implemented to extend the range of application of this optical microrheology technique. Taking advantage of the recently developed "two-cell technique" we show how DWS can be used to investigate the properties of fluid and solid-like complex media. Furthermore, we have significantly extended the range of accessible correlation times to at least 10^{-8}–10^{4} sec using a CCD-based multi-speckle analysis scheme. Excellent agreement is found when comparing the results obtained from DWS to classical oscillatory shear measurements. However, compared to classical rheology, we were able to significantly increase the range of accessible frequencies, thereby opening up a wealth of new possibilities for the study of these fascinating materials.

[1]E-mail: Frank.Scheffold@unifr.ch

1. Introduction

DWS-based optical microrheology uses dynamic light scattering in the multiple scattering regime to obtain information about the viscoelastic properties of soft complex materials (see Refs. [1] and [2] for an overview). This can be done either by direct investigation or by addition of tracer particles to otherwise transparent systems. The underlying idea of optical microrheology is to study the thermal response of small (colloidal) particles embedded in the system under study. Based on the local dynamics, the macroscopic mechanic (viscoelastic) properties are predicted. In recent years, significant progress has been made in development and further understanding about the validity of this approach and its application to fluid and solid soft materials [1]–[12], [16].

Initially, optical microrheology has been mostly restricted to fundamental researchers while it is now becoming increasingly available to both industrial and applied researchers [17]–[20]. One of the most popular techniques to study the thermal motion of the particles is the diffusing wave spectroscopy (DWS), an extension of standard photon correlation spectroscopy (PCS) to turbid media. Here the analysis of (multiply) scattered laser light is used to determine the time evolution of the probe particles mean square displacement [21, 22]. DWS allows access to a broad range of time scales which translates into a large frequency range covered by DWS-based optical microrheology. In this article, we show how modern optical techniques can extend and improve classical rheology both in the sense of frequency range and applicability. Our experiments cover such different materials as polystyrene latex dispersions and gels, giant micelle solutions, as well as ceramic green bodies, casein micellar gels, and biopolymer solutions (for the latter see Refs. [17, 18, 20]) .

2. Diffusing Wave Spectroscopy

Dynamic light scattering (DLS), or photon correlation spectroscopy (PCS), analyzes the fluctuations of the light intensity scattered from a system under study. The light fluctuates due to the local motion of the scatterers. While in "conventional" light scattering experiments the sample has to be almost transparent (and hence often highly diluted), diffusing wave spectroscopy extends conventional dynamic light scattering to media with strong multiple scattering, treating the transport of light as a diffusion process [21, 22]. Provided that the structure factor $S(q) \equiv 1$ (no spatial correlations of the particles) or $k_0 a \gg 1$, it is possible to express the measured intensity autocorrelation function $g_2(\tau) = \langle I(t)I(t+\tau)\rangle \,/\, \langle I\rangle^2$ in terms of the mean square displacement $\langle \Delta \mathbf{r}^2(\tau)\rangle$ of the scattering particle (here $k_0 = 2\pi n/\lambda$ is the wave number of light in a medium with refractive index

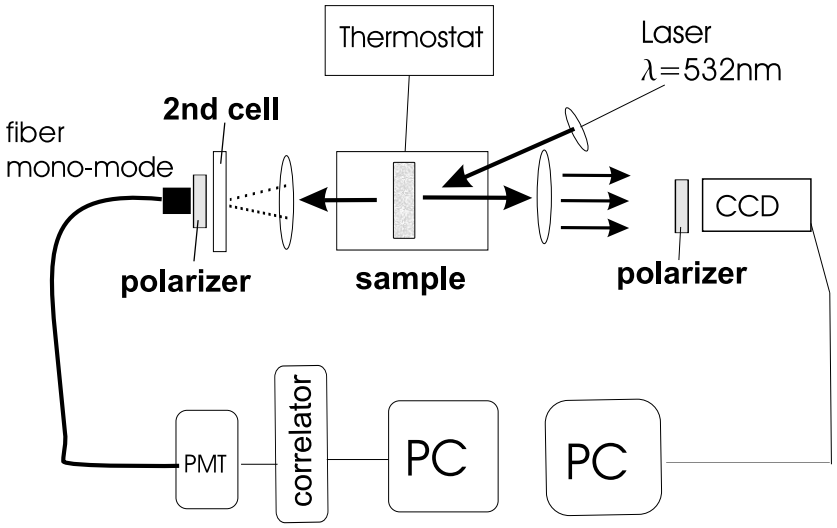

Figure 1. DWS setup: An intense laser beam (Verdi from Coherent) is scattered from a turbid sample contained in a temperature controlled water bath. Two-cell DWS (TCDWS): Light transmitted diffusively from the sample cell is imaged via a lens onto a second cell, containing a highly viscous colloidal suspension of moderate optical density. Subsequently the light is detected with a single mode fiber and analyzed digitally (correlator and PC). Multi-speckle DWS (MSDWS): In backscattering, the fluctuations of the scattered light are analyzed with a CCD camera. MSDWS can also be applied in transmission geometry, in parallel to TCDWS, by placing a beamsplitter between the sample and the lens.

n and a is the particle radius) [21, 22]:

$$g_2(\tau) - 1 = \left| \int_0^\infty ds\, P(s) \exp\left\{ -\frac{1}{3} k_0^2 \left\langle \Delta \mathbf{r}^2(\tau) \right\rangle \frac{s}{l^*} \right\} \right|^2 , \qquad (1)$$

where $P(s)$ is the distribution of photon trajectories of length s in the sample and it can be calculated within the diffusion model taking into account the experimental geometry (typically, transmission or backscattering). The transport mean free path l^* characterizes the typical step length of the photon random walk, given by the individual particles scattering properties and particle concentration. l^* can be determined independently and enters the analysis as a constant parameter. Equation (1) allows one to calculate the particle mean square displacement $\langle \Delta \mathbf{r}^2(\tau) \rangle$ from the measured autocorrelation function $g_2(\tau)$. Figure 1 sketches a typical experimental setup to measure $g_2(\tau)$ both in transmission and backscattering [23]–[25].

2.1. TWO-CELL TECHNIQUE

An important condition for the applicability of the existing theory to PCS experiments is the *ergodicity* of the medium under investigation. Indeed, ensemble-averaged quantities are commonly calculated theoretically, while it is the time averaging which is most easily obtained in experiments. Thus, $\langle \cdots \rangle_E = \langle \cdots \rangle_T$ is required for the experimental data to be described by the theory (where the angular brackets subscripted by E or T stay for the ensemble and time averages, respectively). If the light-scattering sample is nonergodic (say, the sample or some part of it is solid-like), additional efforts are necessary in order to obtain $\langle \cdots \rangle_E = \langle \cdots \rangle_T$ [26]–[28].

To overcome the problem of nonergodicity (arising from the constraint particle motion in a solid like material) in dynamic light scattering, we have recently developed a non-invasive efficient new method [29]. We prepare a system of two independent glass cells (thicknesses L_1 and L_2), where the first cell contains the sample to be investigated, which can be either a stable ergodic or an arrested non-ergodic sample [29]. The second cell, which serves to properly average the signal of the first cell, contains an ergodic, well-characterized system with very slow internal dynamics and moderate turbidity. A nonergodic speckle pattern at the back surface of the first cell (L_1) is imaged via a lens onto the second cell (L_2), as we show schematically in Fig. 1 (see also Refs. [25] and [30]). Transmission through the second cell diffusely broadens the individual speckles to a size $\sim L_2$. Since the second cell is ergodic, a given speckle spot at the back surface of the second cell (and hence the output signal measured by the photomultiplier) is obtained as a result of a two-dimensional average over many speckle spots at the back surface of the first cell. This is equivalent to the ensemble averaging and thus allows us to achieve the required condition of ergodicity $\langle \cdots \rangle_E = \langle \cdots \rangle_T$ for the two-cell system.

The correlation function $g_2(\tau) - 1$ of the two-cell setup can be expressed through the joint distribution function $P_2(s_1, s_2)$ of path segments s_1, s_2 in the cells:

$$\begin{aligned} g_2(\tau) - 1 &= \left| \int_0^\infty ds_1 \int_0^\infty ds_2 \, P_2(s_1, s_2) \exp\left\{ -\frac{1}{3} k_1^2 \left\langle \Delta \mathbf{r}_1^2(\tau) \right\rangle \frac{s_1}{l_1^*} \right\} \right. \\ &\times \left. \exp\left\{ -\frac{1}{3} k_2^2 \left\langle \Delta \mathbf{r}_2^2(\tau) \right\rangle \frac{s_2}{l_2^*} \right\} \right|^2 . \end{aligned} \tag{2}$$

In the case that the cells decouple (i.e. no loops of the scattering paths between the two cells, see Ref. [29] for a more detailed discussion), $P_2(s_1, s_2)$ reduces to a product of two one-cell terms: $P_2(s_1, s_2) = P(s_1)P(s_2)$, and therefore we can write the correlation function of the two-cell setup, $g_2(\tau) - 1$, as a product of the correlation functions of the two independent cells:

$g_2(\tau) - 1 = [g_2(\tau, L_1) - 1] \times [g_2(\tau, L_2) - 1]$ which we call the *"multiplication rule"* (the general theoretical treatment of the two-cell technique is given in Refs. [29] and [31]). We can now directly determine the contribution of the first cell by dividing the signal of the two-cell setup $g_2(\tau) - 1$ by the separately measured autocorrelation function $g_2(\tau, L_2) - 1$ of the ergodic system in the second cell:

$$g_2(\tau, L_1) - 1 = \frac{g_2(\tau) - 1}{g_2(\tau, L_2) - 1}. \tag{3}$$

2.2. MULTI-SPECKLE DWS

Another very useful extension of the standard DWS is the use of a CCD camera to follow temporal fluctuations of the scattered light (see Fig. 1). Instead of analyzing the fluctuations of the intensity at a single spatial position (one speckle spot) we now analyze a large area of the intensity pattern of the scattered light (hence "multi-speckle") using a CCD camera [6, 12, 14, 15]. The main advantage of this setup for the DWS-based microrheology is the significantly improved data acquisition time, since a large number of DWS-scattering experiments is actually performed simultaneously. In the standard DWS (or DLS) measurements, the data acquisition time has to be several orders of magnitude larger than the typical relaxation time of the autocorrelation function $g_2(t) - 1$, a restriction that does not apply to the multi-speckle DWS. Furthermore, since different configurations of the sample are probed simultaneously, the measured autocorrelation function never suffers the problems of nonergodicity described above. The main drawback of the camera-based DWS is the currently still much limited time resolution of CCD cameras. Typically, correlation times τ down to a few ms can be accessed (as compared to 10 ns with a standard photo-multiplier-digital-correlator setup), which is not sufficient for the fast relaxation processes usually encountered in DWS. However, a combination of the novel two-cell technique and multi-speckle DWS, as shown in Fig. 1, turns out to be a perfect one to overcome most of the commonly encountered experimental limitations. Using both techniques allows to cover a temporal range from $\sim$ 10 ns to at least 10^4 sec (the latter being only limited by the "waiting" time), hence more than twelve orders of magnitude in correlation time [12, 13, 25, 30].

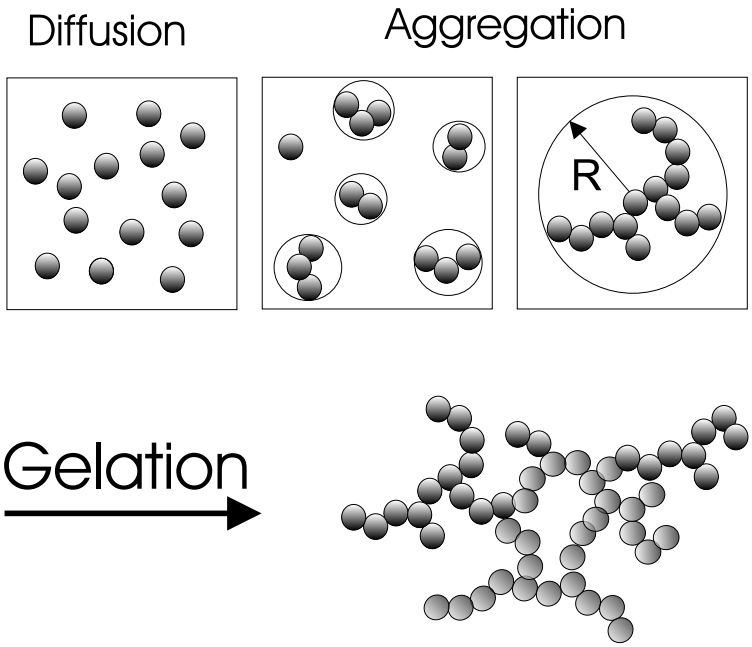

Figure 2. Aggregation and gelation: Attractive inter-particle interactions lead to the growth of individual (fractal) clusters until they fill up the whole accessible volume at $R_c \approx a\,\Phi^{-1/(3-d_f)}$ (Φ is the particle volume fraction).

3. Microrheology

3.1. SOFT SOLIDS: COLLOIDAL AGGREGATES AND GELS

Aggregation and gelation in complex fluids has been for a long time a field of intense research, where both fundamental as well as applied questions are equally important. Applications of gels and sol-gel processing include such different areas as ceramics processing, cosmetics and consumer products, food technology, to name only a few. Gels are formed by chemical or physical reactions of small sub-units (molecules, polymers, or colloids) which can be either reversible or irreversible. The macroscopic features that bring together such different materials are based on the microstructural properties of all gels, which can be described as random networks built up by aggregation of the individual sub-units (see Fig. 2). Starting from a solution of the sub-units, the systems is destabilized, which leads to aggregation, cluster formation, and gelation. At the gel point, a liquid-solid transition is observed which can be characterized by the appearance of a storage modulus

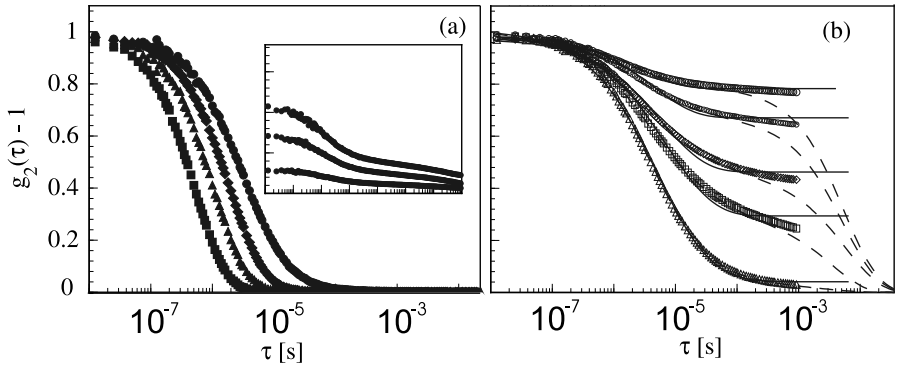

Figure 3. Sol-gel transition in a dense colloidal suspension. Intensity autocorrelation function $g_2(\tau) - 1$ of a two-cell setup during aggregation and gelation at $T = 20°$C. (a) Stable 298 nm suspension (20% vol. fract.) at $t = 0$ min (left curve) and time evolution after destabilization for $t = 11$, 16, 82.5 min (from left to right). Inset: Repeated (time averaged) measurements of $g_2(\tau) - 1$ in the gel state (single cell) show the typical (non-reproducible) nonergodic light scattering signal of a solid-like system. (b) Two-cell correlation function $g_2(\tau, L_1) - 1$ in the gel state after $t = 108$, 256, 734, 4683, 14400 min (from left to right). The solid lines have been recalculated from the fit to the data (see Refs. [7] and [29] for details). The raw-data $g_2(\tau) - 1$ is also displayed (dashed lines).

in rheological measurements. In dilute colloidal gel networks, the individual clusters show a fractal structure leading to a power-law scaling of the structure factor with q: $S(q) \propto q^{-d_f}$ for $a < 1/q < R_c$. The fractal dimension d_f is a measure of the "compactness" of an individual cluster, the higher d_f the more compact the clusters are. For the diffusion-limited cluster aggregation (DLCA) $d_f \simeq 1.8$, while for reaction-limited cluster aggregation (RLCA) $d_f \simeq 2.1$ is expected [32]–[34]. In the most simple picture, the individual clusters grow at a constant rate until they fill up the whole accessible volume, with a critical cluster radius given by

$$R_c \approx a\, \Phi^{-1/(3-d_f)}, \tag{4}$$

where Φ is the particle volume fraction.

Under highly dilute conditions, the structure and dynamics of colloidal gels can be analyzed using single light scattering [35]–[38]. For concentrated colloidal dispersions, we have recently reported the first study of the sol-gel transition based on DWS [7]. In our experiments, a suspension of monodisperse polystyrene latex spheres is destabilized by increasing the solvent ionic strength with a catalytic reaction. Thereby the electrostatic repulsion of the double layer is reduced and the particles aggregate due to Van-der-Waals attraction. Figure 3 shows the measured autocorrelation function as a function of time. At early stages, clusters form due to particle aggregation and

the decay of the correlation function shifts to higher correlation times due to the slower motion of the clusters. Gelation occurs when a single cluster fills the entire sample volume. After the sol-gel transition we observe that the correlation function $g_2(\tau) - 1$ does not decay to zero but remains finite (see Fig. 3). At the "gel time" t_{gel}, the time dependence of the mean square displacement changes qualitatively from diffusion to the arrested motion, being well described by $\langle \Delta \mathbf{r}^2(\tau) \rangle = \delta^2 \{1 - \exp[-(\tau/\tau_c)^p]\}$. At short times $\tau \ll \tau_c$, this expression reduces to a power law: $\langle \Delta \mathbf{r}^2(\tau) \rangle \propto \tau^p$. We find, within our time resolution between different measurements (ca. 1 min), that the exponent for diffusion $p = 1$ drops rapidly at the gel point and takes the value of $p \simeq 0.7$ for all $t > t_{gel}$.

It is furthermore possible to directly link the results of our DWS measurements to the macroscopic storage modulus, taking advantage of a recent model developed by Krall and Weitz [35]. Once the gel spans over the whole sample, the DWS signal is dominated by a broad distribution of elastic gel modes. In the case of fractal (dilute) gels, the storage modulus is given by $G'_0 = G'(\omega \simeq 0) = 6\pi\eta/\tau_c$ [35]. Recently, we have demonstrated that indeed the macroscopic storage modulus G'_0 deduced from the DWS measurements is in a good agreement with the classical rheological measurements over a large range of particle concentrations up to $\approx 10\%$ volume fraction [39].

3.2. VISCOELASTIC FLUIDS: CONCENTRATED SURFACTANT SOLUTIONS

The previous examples addressed systems where the scattering particles are part of the system under study. Now we want to discuss recent measurements where we have introduced tracer particles (polystyrene spheres, diameter 720 nm and 1500 nm) in an otherwise transparent matrix consisting of a concentrated surfactant solution. Under the chosen conditions these surfactants form giant, polymer-like micelles, which results in a surprisingly strong viscoelastic liquid [12, 40]. In this case, we can take advantage of the formalisms derived for the tracer microrheology, which allows to link directly the particle mean square displacement, as obtained from DWS, to the macroscopic viscoelastic moduli $G'(\omega)$ and $G''(\omega)$ [1]–[4]. Figure 4 shows the good agreement between the classical rheology and the DWS-based microrheology, with a dramatically increased frequency range for the latter technique. For a quantitative comparison, a scaling factor of 3/2 has been introduced. The origin of this factor is not well understood yet but, as we think, likely reflects the coupling of the tracer sphere to the medium. Unfortunately, the latter coupling is not understood sufficiently well by current theoretical approaches. In this context, it is interesting to note that the classical Stokes-Einstein relation differs by a very similar factor of 3/2 depending on the choice of the boundary conditions on the particle surface

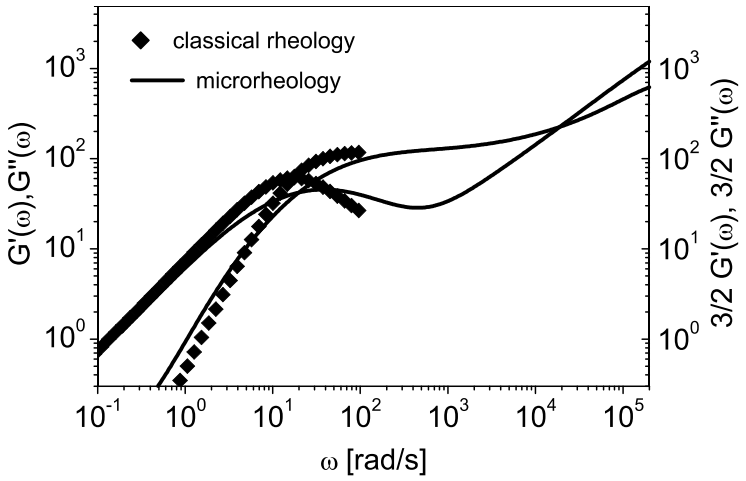

Figure 4. Frequency-dependent elastic moduli of giant micellar solutions (c = 100 mg/ml) at $T = 28°$C obtained from classical rheometry (symbols) and DWS-based microrheology (solid lines, right axis). The microrheology results have been multiplied by a factor 3/2 to allow a quantitative comparison of both experiments. The microrheology results are based on $\langle \Delta \mathbf{r}^2(\tau) \rangle$ data, averaged over two tracer sizes and different particle concentrations ($< 4\%$), thereby reducing statistical errors.

(stick or slip) [41]. Qualitatively similar features have been reported by Starrs and Bartlett in a tracer microrheology study of polymer solutions [42]. However, Bellour *et al.* have found a perfect agreement between the DWS-based microrheology and the classical rheometry for a similar system of worm like micelles [16].

4. Conclusions

In conclusion, we have shown two examples of how dynamic multiple light scattering (diffusing wave spectroscopy, DWS) can be applied to study the mechanical properties of soft complex materials. With the advent of new light scattering techniques, such as the two-cell method, and the use of CCD cameras for slow relaxation processes, it is now possible to apply DWS to an increasingly large number of liquid and solid-like media. This is expected to have an equally strong impact on both applied as well as fundamental research. DWS allows one to obtain the information about the medium rapidly and over a large range of frequencies, which is also of primary importance for many industrial applications, e.g., for rapid system characterization and process monitoring.

References

1. T. Gisler and D.A. Weitz, Curr. Opin. Coll. Int. Sci. **3,** 586 (1998); M.L. Gardel, M.T. Valentine, and D.A. Weitz, in: *Microscale Diagnostic Techniques*, K. Breuer (Ed.) (Springer Verlag, Berlin, 2002), in press.
2. N.J. Wagner and R.K. Prud'homme (Eds.), Curr. Opin. Coll. Int. Sci. **6** (2001).
3. T.G. Mason and D.A. Weitz, Phys. Rev. Lett. **74,** 1250 (1995); T.G. Mason *et al.,* J. Opt. Soc. Am. A **14,** 139 (1997); T.G. Mason *et al.,* Phys. Rev. Lett. **79,** 3282 (1997).
4. F. Gittes, B. Schnurr, P.D. Olmsted, F.C. MacKintosh, and C.F. Schmidt, Phys. Rev. Lett. **79,** 3286 (1997).
5. J.C. Crocker *et al.,* Phys. Rev. Lett. **85,** 888 (2000).
6. A. Knaebel, M. Bellour, J.-P. Munch, V. Viasnoff, F. Lequeux, and J.L. Harden, Europhys. Lett. **52,** 73 (2000).
7. S. Romer, F. Scheffold and P. Schurtenberger, Phys. Rev. Lett. **85,** 4980 (2000).
8. B.R. Dasgupta, S.-Y. Tee, J.C. Crocker, B.J. Frisken, and D.A. Weitz, Phys. Rev. E **65,** 051505 (2002).
9. L.F. Rojas, R. Vavrin, C. Urban, J. Kohlbrecher, A. Stradner, F. Scheffold, and P. Schurtenberger, Faraday Discussions **123,** to appear (2002).
10. K.M. Addas, J.X. Tang, A.J. Levine, C.F. Schmidt, Biophys. J. **82,** 2432 (2002).
11. A.J. Levine and T.C. Lubensky, Phys. Rev. Lett. **85,** 1774 (2000); A.J. Levine and T.C. Lubensky, Phys. Rev. E **63,** 041510 (2000).
12. F. Cardinaux, L. Cipelletti, F. Scheffold, and P. Schurtenberger, Europhys. Lett. **57,** 738 (2002).
13. F.A. Erbacher, R. Lenke, and G. Maret, Europhys. Lett. **21,** 551 (1993).
14. S. Kirsch, V. Frenz, W. Schartl, E. Bartsch, and H. Sillescu, J. Chem. Phys. **104,** 1758 (1996).
15. L. Cipelletti, S. Manley, R.C. Ball, and D.A. Weitz, Phys. Rev. Lett. **84,** 2275 (2000).
16. M. Bellour, M. Skouri, J.P. Munch, and P Hebraud, Eur. J. Phys. **8,** 431 (2002).
17. P. Schurtenberger, A. Stradner, S. Romer, C. Urban, and F. Scheffold, CHIMIA **55,** 155 (2001).
18. H. Wyss, S. Romer, F. Scheffold, P. Schurtenberger, and L.J. Gauckler, J. Coll. Int. Sci. **241,** 89 (2001).
19. A.J. Vasbinder, P.J.J.M. van Mil, A. Bot, and K.G. de Kruif, Coll. and Surfaces B — Biointerfaces **21,** 245 (2001).
20. C. Heinemann, F. Cardinaux, F. Scheffold, P. Schurtenberger, F. Escher, and B. Conde-Petit, Tracer microrheology of γ-dodecalactone induced gelation of aqueous starch systems, in preparation.
21. G. Maret and P.E. Wolf, Z. Phys. B **65,** 409 (1987).
22. D.A. Weitz and D.J. Pine, in: *Dynamic Light Scattering,* W. Brown (Ed.) (Oxford Univ. Press, New York, 1993), Chap. 16.
23. Figure 1 schematically dispays the most recent and advanced DWS setup installed in Fribourg. The different setups used in the actual experiments are similar but not identical. For details we refer to the original papers (references given in this article).
24. F. Scheffold, J. of Disp. Sci. and Tech. **23,** 591 (2002).
25. H. Bissig, S. Romer, L. Cipelleti, V. Trappe, and P. Schurtenberger, Intermittent dynamics and hyper-aging in dense colloidal gels, submitted to PhysChemComm (e-journal).
26. J.Z. Xue, D.J. Pine, S.T. Milner, X.L. Wu, and P.M. Chaikin, Phys. Rev. A **46,** 6550 (1992); P.N. Pusey and W. van Megen, Physica A **157,** 705 (1989).
27. G. Nisato, P. Hébraud, J-P. Munch, and S.J. Candau, Phys. Rev. E **61,** 2879 (2000).
28. M. Heckmeier and G. Maret, Progr. Colloid Polym. Sci. **104,** 12 (1997); Opt. Commun. **148,** 1 (1998).
29. F. Scheffold, S.E. Skipetrov, S. Romer, and P. Schurtenberger, Phys. Rev. E **63,**

061404 (2001).
30. V. Viasnoff, F. Lequeux, and D.J. Pine, Rev. Sci. Instrum. **73,** 2336 (2002).
31. S.E. Skipetrov and R. Maynard, Phys. Lett. A **217,** 181 (1996).
32. D.A. Weitz and M. Oliveria, Phys. Rev. Lett. **52,** 1433 (1984); D.A. Weitz, J.S. Huang, M.Y. Lin, and J. Sung, Phys. Rev. Lett. **53,** 1657 (1984); P. Dimon, S.K. Sinha, D.A. Weitz, C.R. Safinya, G.S. Smith, W.A. Varady, and H.M. Lindsay, Phys. Rev. Lett. **57,** 595 (1986); R. Klein, D.A. Weitz, M.Y. Lin, H.M. Lindsay, R.C. Ball, and P. Meakin, Prog. Coll. Int. Sci. **81,** 161 (1990).
33. E. Dickinson, J. Coll. Int. Sci. **225,** 2 (2000) and references therein.
34. C.M. Sorensen, Aerosol Sci. Tech. **35,** 648 (2001).
35. A.H. Krall and D.A. Weitz, Phys. Rev. Lett. **80,** 778 (1998).
36. D.W. Schaefer, J.E. Martin, P. Wiltzius, and D.S. Cannell, Phys. Rev. Lett. **52,** 2371 (1984); Dietler and D.S. Cannell, Phys. Rev. Lett. **60,** 1852 (1988).
37. M. Carpineti and M. Giglio, Phys. Rev. Lett. **68,** 3327 (1992).
38. T. Nicolai, D. Durand, and J. Gimel, Phys. Rev. B **50,** 16357 (1994).
39. H. Bissig, S. Romer, V. Trappe, F. Scheffold, and P. Schurtenberger, unpublished.
40. J.D. Ferry, *Viscoelastic Properties of Polymers*, 3rd ed. (John Wiley and Sons, New York, 1980).
41. J.-P. Hansen and I.R. McDonald, *Theory of Simple Liquids* (Academic Press, London, 1996).
42. L. Starrs and P. Bartlett, Faraday Discussions **123,** to appear (2002).